sustainability

MDPI

Article

Seismic Response of a PC Continuous Box Girder Bridge under Extreme Ambient Temperature

Li Wang [1,2,*], Lusong Yu [1], Xinlong Du [1], Xiyin Zhang [1] and Ziqi Li [1]

[1] School of Civil Engineering, Lanzhou Jiaotong University, Lanzhou 730070, China; zhangxiyin@lzb.ac.cn (X.Z.)
[2] Gansu Gonghang Travel Road Industry Co., Ltd., Lanzhou 730030, China
* Correspondence: wangli1993@mail.lzjtu.cn

Abstract: To study the effect of temperature on the seismic performance of a prestressed reinforced concrete (PC) continuous girder bridge with laminated rubber bearings (LRBs), a two-linked continuous bridge was used as the background to consider the effect of extreme temperature on the properties of LRBs and pier concrete. First, the properties of concrete specimens were tested at different temperatures to obtain their mechanical parameters at extreme temperatures. Then, we obtained the effect of extreme temperature on the seismic response of consecutive bridges with LRBs by examining the seismic response of the pier moments, pier top displacements, and bearing deformations. The results show that compared with normal temperatures, the extreme temperature causes a change in parameters of the LRBs and concrete pier, which increases the internal force and displacement response of a pier under an extremely low temperature by 37.13% and 32.74%, respectively. The displacement of bearings under extremely high temperature conditions increases by 16.31%. The influence of temperature changes on the mechanical parameters of LRBs will change the connection stiffness of the pier and superstructure, resulting in significant changes in the seismic response of the pier and bearing, so that the internal force and displacement response of the pier are negatively correlated with the temperature.

Keywords: extreme temperature; laminated rubber bearing; constitutive relation; bearings stiffness; continuous box girder bridge; seismic response

Citation: Wang, L.; Yu, L.; Du, X.; Zhang, X.; Li, Z. Seismic Response of a PC Continuous Box Girder Bridge under Extreme Ambient Temperature. *Sustainability* **2023**, *15*, 14763. https://doi.org/10.3390/su152014763

Academic Editor: Humberto Varum

Received: 29 August 2023
Revised: 4 October 2023
Accepted: 7 October 2023
Published: 11 October 2023

1. Introduction

Prestressed concrete continuous girder bridges have the advantages of little deformation, high structural stiffness, smooth and comfortable travel, small expansion joints, convenient maintenance, strong seismic resistance, etc. They have obvious advantages as small and medium-sized span bridges. At present, they have been widely used in bridge construction nationwide and abroad [1,2]. The climate temperature difference in China is large: the winter temperature in the northwest is low and the winter temperature in most parts of the northeast and northwest is below −10 °C. Due to long-term exposure to the atmospheric environment, the bridge structure is directly affected by the atmospheric temperature, and the action of extreme ambient temperature leads to large displacement and structural internal force of the bridge structure [3–5], affecting the modal change of the bridge [6,7]. The bridges in these areas not only need to be designed for vibration reduction and isolation to reduce the damage caused by earthquakes [8], but also need to consider the impact of extreme temperatures on the bridge structure. At present, the research on the seismic performance of bridges under the influence of ambient temperature has been mainly focused on the changes in the seismic response of bridges due to changes in the performance of bridge bearings under the influence of temperature at home and abroad. Scholars at home and abroad have conducted many useful studies on parameters such as equivalent stiffness [9–11], yield force [12–14], compressive strength [15,16], frictional slip

properties [17,18], and damping characteristics [19] of plate rubber bearings at different ambient temperatures, and systematically explored the correlation between each of these parameters and the ambient temperature. A bridge structure with plate rubber bearings is exposed to the external environment for a long time, and the ambient temperature will inevitably lead to changes in the mechanical behavior of the bearings, resulting in a change in the dynamic characteristics of the bridge structure. In view of the above problems, Du et al. [20] and Billah et al. [21] explored the influence of low temperatures on the main performance of rubber isolation devices and the seismic responses of isolation structures through a numerical simulation method. Through a review of the current state of research, it was found that scholars have carried out extensive research on the mechanical properties of laminated rubber bearings affected by temperature and their impact on the seismic performance of bridges, and achieved some research results. However, the research shows that temperature not only has an impact on the mechanical properties of rubber bearings, but also has a significant impact on the strength, elastic modulus, and peak strain of pier concrete materials [22,23]. Li et al. [24] discussed the compression peak strain and stress-strain relationship curve of a freeze-thaw cycle of −20 °C~20 °C through experiments. The results show that the dynamic mechanical properties of concrete under a freeze-thaw environment are the comprehensive result of the freeze-thaw deterioration effect and strain rate strengthening effect. Krishna et al. [25] studied the mechanical properties of concrete at high temperatures. The structure they studied shows that the peak strain of concrete increases with an increase in temperature. Due to the increase in temperature, the compressive strength of concrete decreases and the ductility increases, so that the slope of the stress-strain curve decreases with the increase in temperature. Xie et al. [26,27], Li et al. [28], and Yan et al. [29] found that when the temperature decreases, the peak stress and elastic modulus of concrete increase, while the peak strain and ductility show an approximately linear decreasing trend. At present, the existing research mainly focuses on the influence of ambient temperature on the mechanical properties of rubber bearings. However, as a vulnerable component under earthquakes, the stiffness of piers under different ambient temperatures also affects the seismic performance of structures. To sum up, it is necessary to study the seismic performance of isolated bridge structures under different ambient temperatures and considering the influence of pier concrete and bearing stiffness.

Based on existing research results, this paper uses MIDAS/Civil software to analyze the seismic response of a two-linked 3 × 32 m PC continuous box girder bridge by simultaneously considering the effect of temperature on the mechanical parameters of the concrete materials of the bearings and piers, and to compare and analyze the characteristics of the effect of temperature on the seismic performance of this type of continuous girder bridge according to the seismic response of bearing displacement and pier internal force.

2. Establishment of a Numerical Model

2.1. Engineering Background and Finite Element Modeling

The bridge is located on an expressway in Qinghai Province. The bridge span is arranged in two 3 × 32 m continuous box girder bridges. The superstructure is made of prestressed concrete box girders with a height of 1.6 m. The substructure consists of double-column rectangular piers with C40 concrete, and the middle pier consists of a (1.3 × 1.6) m section and the intersection pier consists of a (1.8 × 1.8) m section. The structure below the ground adopts the form of a pile foundation, with four piles of 1.5 m diameter under each pier, and the pile foundation is C30 concrete and the length of each pile is 50 m. The bearings are GYZd500-type natural rubber bearings (No.1~24). The bridge site is located in the cold area of the plateau, where the extreme high and low temperatures are set at 40 °C and −40 °C respectively.

The GYZF4600 × 150 mm bearings were adopted on bent caps. The GYZd800 × 148 mm bearings were adopted on the bridge piers. The specific specifications and parameters are shown in Table 1.

Table 1. Specification parameters of the laminated rubber bearings.

Bearing Type	Maximum Bearing Force (R_{ck}/kN)	Shape Factor(S)	Bearing Thickness (t/mm)	Rubber Layer Thickness (t_e/mm)	Minimum Anti Slip Bearing Pressure (R_{GK}/kN)	Intermediate Rubber Layer Thickness (t_1/mm)	Single Layer Steel Plate Thickness (t_0/mm)
GYZF4600	2 734	9.83	150	110	990	15	5
GYZd800	4 902	10.97	148	113	1759	18	5

The nonlinear finite element model of the bridge was established by MIDAS Civil software. The beam was simulated by the elastic beam element. The pier was simulated by the nonlinear fiber beam element. The constrained (non-constrained) concrete of the piers was simulated by the Mander model. The main reinforcement was simulated by the double broken line model. The finite element model of the whole bridge is shown in Figure 1 and 1#~24# is the plate rubber bearing. The node at the bottom of each pile restricts the degrees of freedom in six directions. The mechanical model of the plate rubber bearing is greatly different from the commonly used linear model of rubber bearing after the friction and slip of the plate rubber bearing under the action of an earthquake. Finally, the bilinear hysteretic model was used to simulate the friction and slip performance of the plate rubber bearing between the contact surface of the pier tops and beam bottoms.

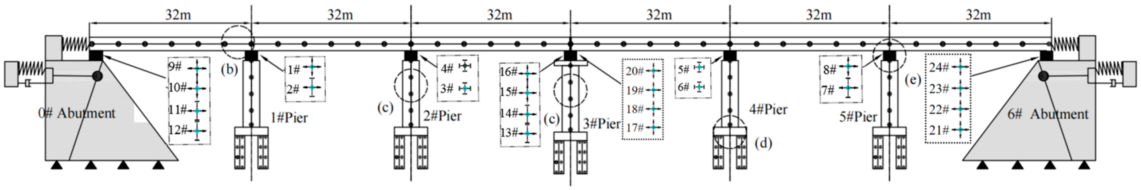

(**a**) Overall layout of the bridge

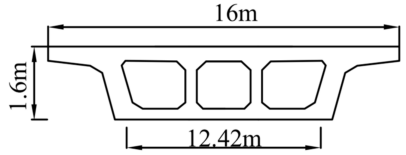

(**b**) Main beam section

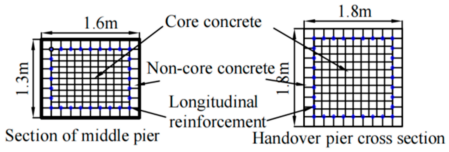

(**c**) Pier fiber section

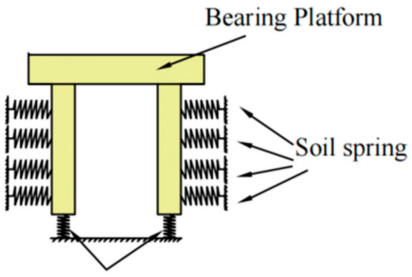

(**d**) Support springs

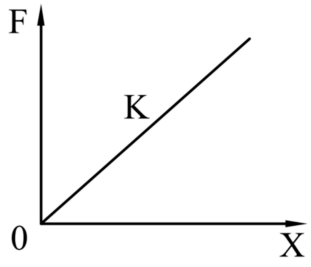

(**e**) Mechanical model of Laminated rubber bearing

Figure 1. Finite element model of bridge.

2.2. Experimental Program

2.2.1. Bridge Pier Parameters

For the constitutive relationship of concrete, the important parameters in the Mander model are concrete compressive strength, elastic modulus, and peak strain. In order to further study the influence of temperature on the properties of the concrete materials, a batch of mechanical property tests of concrete prismatic specimens at different temperatures were carried out for this paper.

(1) Test overview

A total of 12 prismatic concrete specimens (including 3 spares) were prepared in this experiment, with a size of 150 mm × 150 mm × 300 mm and a design strength of C40. Ordinary Portland cement was used, and the specimens were cured for 28 days. The influence of the temperature parameters was mainly considered: the specimens were grouped into A1 to A3 and the corresponding temperatures were 40 °C, 20 °C, and −40 °C, respectively. In this test, temperature sensors were arranged in the nine prism test blocks. The sensors were stainless steel PT100 temperature sensors, with an accuracy of ±0.5 °C, measurement range of −50 °C~125 °C, stability of ±0.5 °C, and linear error of ±0.3 °C. An intelligent temperature regulator was used for data acquisition.

To carry out the compressive test of the concrete prisms at different temperatures, it was first necessary to solve the problems of heating, cooling, and heat preservation of the specimens. For the high and low temperature environment simulation, this study used a low temperature refrigerator and an electric heat tracer to provide the required temperatures; the temperature test verification showed that the temperature difference between the specimen temperature and the design temperature was within ±2 °C, which ensured a relatively stable temperature condition during the test. The test was carried out in a 300-ton pressure testing machine. During the low-temperature test, each specimen used for the low-temperature test was first frozen in a refrigerator to provide a low-temperature environment. The sensors were set in the center of the concrete specimen and in the refrigerator. During the process, the central temperature of the specimen and the ambient temperature in the refrigerator were measured in real time. According to the specification "Technical Specifications for Concrete Application in Low Temperature Environment" (GB 51081−2015) [30], before the test, each test block was kept in the refrigerator for 48 h. First the ambient temperature was cooled to the test temperature, and finally the center temperature of the concrete specimen reaching the target temperature point was the sign that the test was entering the temperature-holding state. The high-temperature test was similar. First, each specimen used for the high-temperature test was wrapped with a heating cable, and then heated by electricity. Finally, the center temperature of the concrete specimen reaching the target temperature point was the sign that the test was entering the temperature-holding state. During the heating and cooling process, the central temperature of a temperature specimen under the same conditions was monitored in real time. The specific lifting equipment and loading equipment are shown in Figure 2.

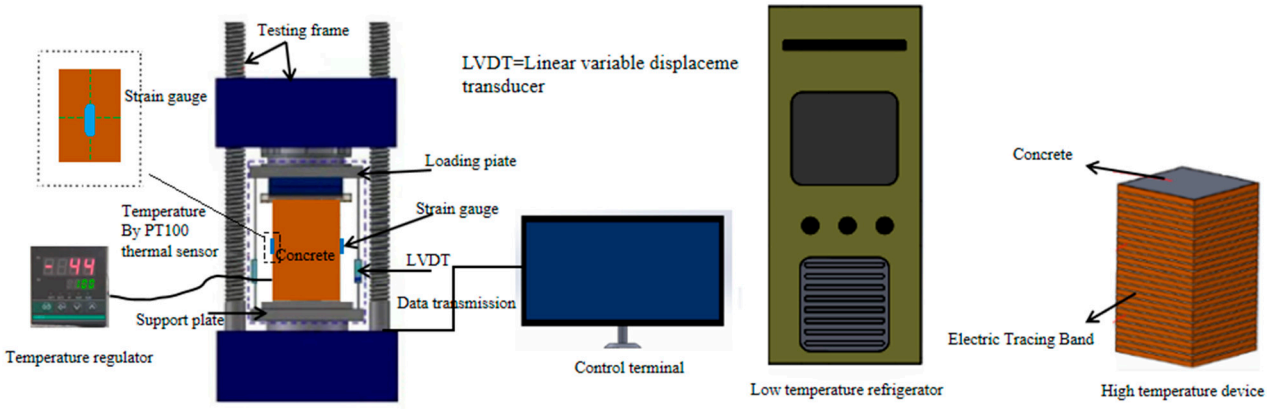

Figure 2. High and low temperature devices and loading equipment.

(2) Loading scheme

Referring to the loading method at normal temperature, the constitutive relationship test of concrete under high and low temperature environments also adopted equal stress rate loading, and the loading rate was controlled at about 10 με/s until the damage occurred in the specimen. During the test, the load was directly controlled by the YAW4306

microcomputer-controlled electro-hydraulic servo pressure testing machine. Considering that the concrete at the end of the test piece would be restrained by a certain hoop, the pure compression section in the middle of the test piece was selected as the strain measurement area, and the strain was determined by the test piece. BF120-30AA foil resistance strain gauges on both sides of the piece were measured. The strain gauges were connected to the corresponding measurement channel of the YE2533 resistance strain gauge using a 1/4 bridge, and its measurement accuracy is 0.002 mm/με.

(3) Experimental phenomena

Under a normal temperature (20 °C), when the load is $0.8f_c$~$0.9f_c$, a small vertical crack started to appear in the middle area of the specimen, and the crack was parallel to the direction of force (Figure 3b). With an increase in the load, the crack gradually developed until it penetrated the whole specimen, the specimen was damaged, and the experiment was ended. Considering temperature dissipation, when the low temperature test was carried out, the initial temperature was set to about −42 °C (the design temperature was −40 °C) and wrapped with thermal insulation cotton for insulation. Under the premise of equal speed loading, the damage of the specimen was more violent than that at room temperature, and a larger damage sound was issued, because the ultimate strain of concrete is reduced at low temperatures, and the test time became shorter when equal speed loading was used (Figure 3c). Meanwhile, the high temperature (40 °C) test showed the opposite phenomenon (Figure 3a). The damaged specimens are shown in Figure 3.

(**a**) 40 °C (**b**) 20 °C (**c**) −40 °C

Figure 3. Concrete prism failure mechanisms at different temperatures.

It can be seen from Figure 3c that at −40 °C, the specimen was sheared and damaged seriously, with an oblique main crack running through the cross-section, and the crack width was large. Meanwhile, at 40 °C, several fine cracks emerged in the specimen which gradually developed through the entire test piece causing the failure of the test piece.

(4) Analysis of test results

By summarizing and analyzing the concrete stress-strain curves under different temperature conditions, the variation trend of the concrete stress-strain curves with temperature(40 °C, 20 °C, −40 °C) can be obtained as shown in Figure 4.

It can be seen from Figure 4 that in the ascending section of the stress-strain curves, as the temperature decreases, the slope of the curve increases, the stress of the specimen increases more rapidly, and the bearing capacity value of the specimen increases gradually, indicating that the concrete strength decreases. The elastic modulus gradually increased, and the trend of the curve was consistent with the literature [31,32]. The descending section of the curve becomes steeper and shorter and disappears gradually with the decrease in temperature, indicating that the brittleness of the concrete increases gradually with the decrease in temperature.

In order to further quantitatively analyze the relationship between the three temperatures, the peak stress, strain and secant modulus at $0.5f_c$ of each specimen at different

temperatures are summarized in Table 2. The average value of the results of each group of three specimens is taken as the final result of the group of specimens.

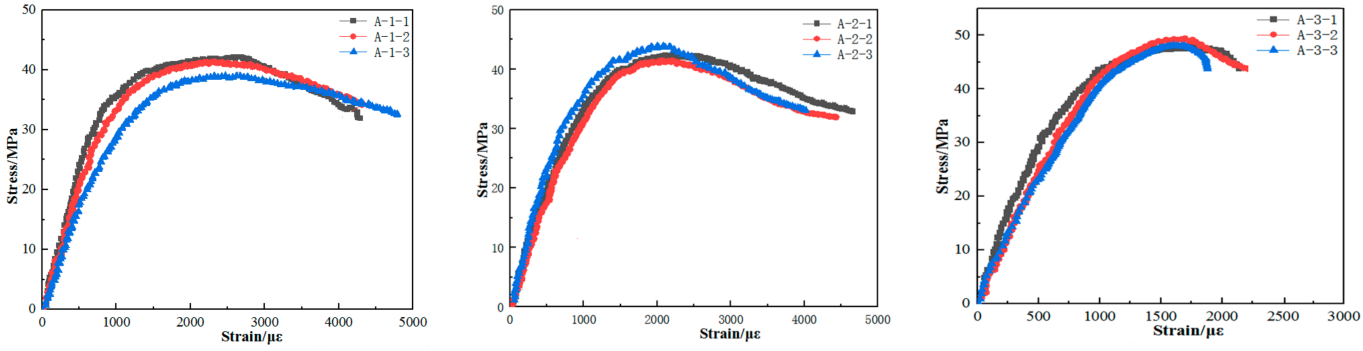

(**a**) 40 °C (**b**) 20 °C (**c**) −40 °C

Figure 4. Concrete stress-strain curves under different temperatures.

Table 2. Average value of peak stress and corresponding strain in each specimen.

Specimen Groups	Test Temperature (°C)	Design Strength (MPa)	Peak Stress (MPa)	Peak Strain (με)	Modulus of Elasticity (GPa)
A-1	40	C40	40.52	2661	43.53
A-2	20	C40	42.76	2259	45.67
A-3	−40	C40	48.45	1689	51.15

Note: The modulus of elasticity in the table is the cut-line modulus corresponding to $0.5f_c$.

Since the compressive strength of Mander constitutive concrete is the compressive strength of the cylinder, it is necessary to multiply the concrete strength obtained in the test by a correction factor of 0.85. The values of the mechanical properties are shown in Table 3.

Table 3. Material properties of concrete and steel bars.

Materials	Properties	Temperature/°C		
		40	20	−40
Concrete	Compressive strength (MPa)	34.44	36.35	41.18
	Tensile strength (MPa)	3.33	3.33	3.33
	Modulus of elasticity (MPa)	43,533.04	45,676.17	51,154.70
	Peak strain (με)	2661	2259	1689
Reinforcement	Modulus of elasticity (MPa)	196	196	196
	Yield stress (MPa)	468	479	512
	Ultimate stress (MPa)	692	692	692

Regarding the constitutive model of concrete at room temperature, many scholars at home and abroad have proposed a variety of compressive stress-strain curve equations, typically Szenz's polynomial model, Sahlin, Smith, and Young's exponential model, and Young's trigonometric function model. In the 1980s, Guo et al. [33] of Tsinghua University proposed to use dimensionless stress and dimensionless strain as the x-axis and y-axis, respectively, to fit the stress-strain curve of concrete in sections. The mathematical expression is as follows:

$$\begin{aligned} y &= Ax + (3-2A)x^2 + (A-2)x^3, 0 < x < 1 \\ y &= x\left[a(x-1)^2 + x\right]^{-1}, x > 1 \end{aligned} \quad (1)$$

where the parameter A of the ascending section represents the ratio of the initial elastic modulus of the concrete to the secant modulus of the concrete at the peak point, while a

represents the steepness of the descending section to a certain extent, that is, it is positive with the absolute value of the stiffness of the related descending section. In this paper, the curve fitting expression of Guo et al. is used to numerically analyze the curve parameters, and the undetermined parameters of the ascending and descending sections of the concrete stress-strain curve at different temperatures are obtained, which are summarized in Table 4.

Table 4. Summary of values of A and a.

Temperature (°C)	40	20	−40
A	2.86	2.42	1.78
a	0.7	1.3	2.0

Taking the peak stress and peak strain of concrete at the extreme temperatures obtained in Table 4 and multiplying them by the corresponding x and y, respectively, using Equation (7), the principal structure relationship curves of the concrete of this bridge pier at different temperatures can be obtained in Figure 5.

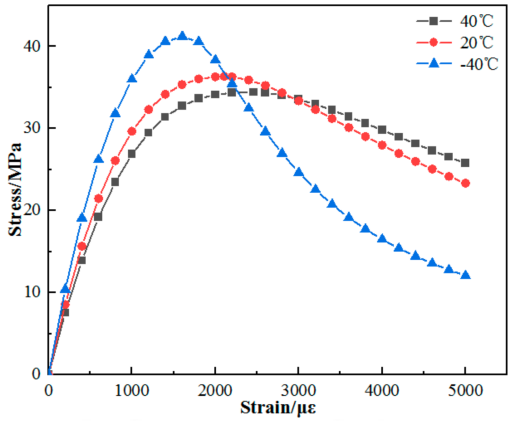

Figure 5. Theoretical stress-strain curves of concrete at different temperatures.

2.2.2. Bridge Pier Reinforcement

Regarding the influence of extreme temperatures on the mechanical parameters of steel bars, Yan et al. [34] and Xie Jian et al. [35] conducted tensile tests on 21 groups of 63 specimens of HRB335, HRB400, and special low-temperature steel bars at 20 to −165 °C. They showed that, compared with the yield strength at normal temperature (20 °C), the yield strength of the various steel bars increases by 7.2%, 1.5%, and 3.5% at −40 °C, respectively; the tensile strength increases by 4.1%, 4.0%, and 10.1%, respectively; while the change in the elastic modulus of the steel bars at extreme temperatures does not exceed 3.0% at −40 °C. The elastic modulus of the three steel bars has little correlation with temperature, and its value basically fluctuates around a certain value. Since HRB400 is used for the reinforcement of the bridge, combined with the existing research, it is found that the extreme temperature has little effect on its mechanical parameters, so this paper does not consider the influence of temperature on the mechanical properties of the bridge pier reinforcement.

2.2.3. Bearing Parameters

Due to the thermal sensitivity of rubber, the compressive elastic modulus E and shear modulus G change with temperature. For the relationship between the bearing performance and temperature, Zhuang et al. [36] gave the bearing performance test data of laminated rubber bearings between −50 °C and 15 °C, with the bearing stiffness at 18 °C as the benchmark. Jin et al. [37] completed performance tests between −10 °C and 40 °C, using a 20 °C bearing stiffness as a benchmark. Based on the two, the temperature influence coefficients of the laminated rubber bearings at 40 °C, 20 °C and −40 °C were obtained by

conversion, as shown in Table 1. And for the simulation of the laminated rubber bearings in the finite element software, six parameters were required, namely, SDx, SDy, SDz, SRx, SRy, and SRz.

Parameters in the X-axis direction:

$$SDx = \frac{EA}{L} \tag{2}$$

Stiffness in the Y and Z axes directions:

$$SDy = SDz = \frac{GA}{L} \tag{3}$$

The rotation stiffness around the X-axis direction is:

$$SRx = \frac{GI_P}{L} \tag{4}$$

The rotational stiffness in the direction of the Y and Z axes is:

$$SRy = \frac{GI_y}{L} \tag{5}$$

$$SRz = \frac{GI_z}{L} \tag{6}$$

where E is the bearing compressive modulus of elasticity, G is the bearing shear modulus of elasticity, A is the cross-sectional area, L is the height of the bearing, t_e, in the calculation of the stiffness, L is the total thickness of the rubber layer of the bearing, I_y and I_z are the cross-sectional bending moments of inertia, and I_p is the cross-sectional torsional moment of inertia.

According to "Highway Bridge Plate Rubber Bearing" (JTT4-2019) [38]:

$$E = 5.4GS^2 \tag{7}$$

$$S = \frac{d_0}{4t_1} \tag{8}$$

where S is the shape coefficient of the bearing, t_1 is the thickness of the single-layer rubber sheet in the middle of the bearing, and d_0 is the diameter of the stiffened steel plate of the circular bearing.

Based on the Formulas (2) to (8), the parameters of the plate rubber bearing at different temperatures are calculated as shown in Table 5.

Table 5. Parameters of laminated rubber bearings under extreme temperatures.

Parameters	40 °C	20 °C	−40 °C
Temperature influence coefficient τ	0.9432	0.997	1.6098
Shear modulus *G* (MPa)	0.9432	0.997	1.6098
Compressive elastic modulus E (MPa)	339.9708	359.3627	580.2429
Vertical stiffness SDx/(kN·m^{-1})	577,681.6199	610,632.5011	892,313.4109
Horizontal stiffness SDy, SDz/(kN·m^{-1})	1704.77317	1802.0132	2874.436
Horizontal rotation stiffness SRx/(kN·m·rad^{-1})	52,348,819.15	55,334,788.69	88,265,896.58
Vertical rotation stiffness SRy, SRz/(kN·m·rad^{-1})	8.669×10^9	9.163×10^9	1.339×10^{10}

3. Selection of Ground Vibration

The characteristic period of the earthquake zone where the bridge site is located is 0.4 s, the site category is Class II, and the seismic fortification intensity is VII (0.1 g). The key to calculating and simulating a bridge earthquake is to select appropriate seismic

waves. In order to accurately explore the seismic performance of the laminated rubber bearings of continuous girder bridges under extreme temperatures, the response spectrum characteristics of the design response spectrum at the bridge site were selected from the Pacific Earthquake Engineering Research (PEER) Center in the United States. The seven seismic waves that are close to each other are studied on the background bridge, and the seismic acceleration response spectrum is shown in Figure 6, the different colored curves represent the different seismic waves selected.

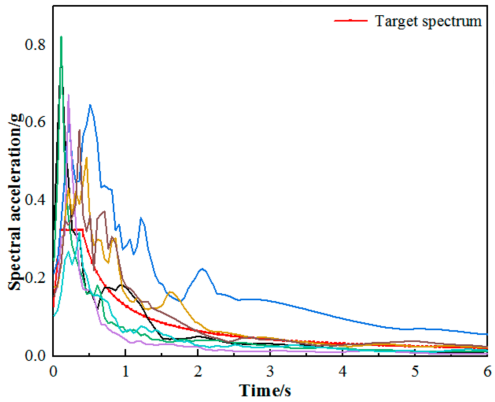

Figure 6. Ground motion spectrum.

4. Seismic Response Analysis

4.1. Load Conditions

In order to investigate the effect of extreme temperature action on the seismic response of continuous beam bridges with plate rubber bearings, the analysis will be carried out using the load conditions in Table 6. In addition, the presence of vehicle loads on the bridge is not considered during the calculation.

Table 6. Load cases.

Case Conditions	Temperature/°C	Temperature Influence Parameters	
1	Normal temperature (20)	-------	-------
2	Extreme high temperature (40)	-------	Laminated rubber bearing
3	Extreme high temperature (40)	Bridge pier	Laminated rubber bearing
4	Extreme low temperature (−40)	-------	Laminated rubber bearing
5	Extreme low temperature (−40)	Bridge pier	Laminated rubber bearing

4.2. Analysis of Results

In accordance with the "China Earthquake Parameter Zoning Map" (GB 18306—2015) [39], this paper modulates the amplitude of seven ground motion records to E1 earthquakes (PGA is 0.1 g), E2 earthquakes (PGA is 0.3 g), and extremely rare earthquakes (PGA is 0.6 g). It analyzes the seismic response of the bridge in the transverse direction and along the bridge direction under different ground motion intensities and different calculation conditions and studies the bending moment at the bottom of each pier, the displacement at the top of the pier, and the deformation of the bearing response law.

Analysis of Seismic Response along the Bridge

(1) Pier bottom bending moments

From the pier bottom bending moment ratio diagram (Figure 7) obtained from the extreme temperature conditions (conditions 2 to 5) and the normal temperature condition (condition 1) of the bridge under the action of the bridge-direction earthquake, it can be seen that under the seismic action in the parallelogram direction, the support stiffness, concrete modulus of elasticity, and other parameters are affected by the extreme temperatures.

The pier bottom bending moment changes significantly from the normal temperature, the overall performance of the pier bottom bending moment for extreme low temperature conditions (conditions 4,5) > normal temperature conditions (condition 1) > extreme high temperature conditions (conditions 2,3), and the larger the PGA, the more obvious the law. When only considering the influence of the mechanical properties of the rubber bearings on the seismic performance of the bridge at extreme temperatures, comparing working conditions 1, 2, and 4 and PGAs of 0.1 g (Figure 7a), 0.3 g (Figure 7b), and 0.6 g (Figure 7c), it was found that the response of the pier bottom bending moment at different temperatures is quite different. Compared with that in condition 1, the pier bottom bending moment in condition 4 was increased by 28.3%, 29.6%, and 31.3% when the PGA was 0.1 g, 0.3 g, and 0.6 g, respectively. In case 1, the maximum decrease was 2.39%, 2.42%, and 8.69%, respectively. In the low temperature environment it was found that when the PGA was 0.1 g, 0.3 g, and 0.6 g, the bending moment of the pier bottom in working condition 5 was increased by 5.94%, 8.51%, and 10.25%, respectively, compared with working condition 4. This is due to the increase in the stiffness of the pier due to the decrease in the temperature, the increase in the strength and elastic modulus of the concrete, and the decrease in the peak strain. For the 3# junction pier, when the PGA was 0.10 g, the bending moment under the extreme low temperature condition (condition 5) increased by 31.63% compared with the normal temperature condition (condition 1), and increased by 32.53% when the PGA was 0.30 g and 37.13% when the PGA was 0.6 g. From the observation of the bending moment changes of the 1#~5# bridge piers in the figure, it can be seen that with the increase in the ground motion intensity, the bending moment of the 3# junction pier changes obviously. However, the increase for the other piers is not more than 25%, which is mainly because the junction pier is used as a bridge pier shared by two adjacent bridges. Under the action of the seismic force along the bridge, the displacement of the superstructure and the deformation of the bearing cause the junction pier to generate additional forces and the additional bending moment causes the change in the bending moment at the bottom of the 3# pier.

(2) Displacement of pier tops

From the pier top displacement ratio diagram (Figure 8) obtained under extreme temperature conditions and normal temperature conditions for the bridge under the action of earthquakes along the bridge, it can be seen that compared with conditions 1~5, the connection stiffness between the upper and lower parts of the bridge increases due to the decrease in temperature. Therefore, the pier top displacement under low temperature conditions is significantly greater than that under normal temperature and high temperature conditions. In the low temperature state, due to the decrease in temperature, the pier concrete strength and elastic modulus increase and the peak strain decreases, resulting in the increase in its own stiffness. Therefore, the pier top displacement in condition 5 is lower than that in condition 4, and the maximum decrease was 3.50%, 7.88%, and 10.35% when the PGA was 0.10 g (Figure 8a), 0.30 g (Figure 8b), and 0.60 g (Figure 8c), respectively. And the opposite is true for the high temperature condition. Only considering the influence of the mechanical properties of the rubber bearings under extreme temperatures, comparing the working conditions 1, 2 and 4, it can be seen that under the effect of different seismic excitation, the displacement of the top of the pier in working condition 4 increased by 37.56%, 34.20%, and 42.68%, respectively, and the increase increased from anywhere to the peak acceleration of vibration. The displacement of the top of the pier in working condition 2 decreased by 8.91%, 7.05%, and 9.20%, respectively, and the decrease rate decreased when the peak acceleration of vibration increased. It is observed that, comparing case 4 and case 5, the displacement of the pier top of piers 2 and 4# changed obviously compared with other piers, and changed by 3.50%, 7.88%, and 10.35%, respectively, under the different seismic intensities. This is mainly due to the fact that the pier bottom supports are fixed supports.

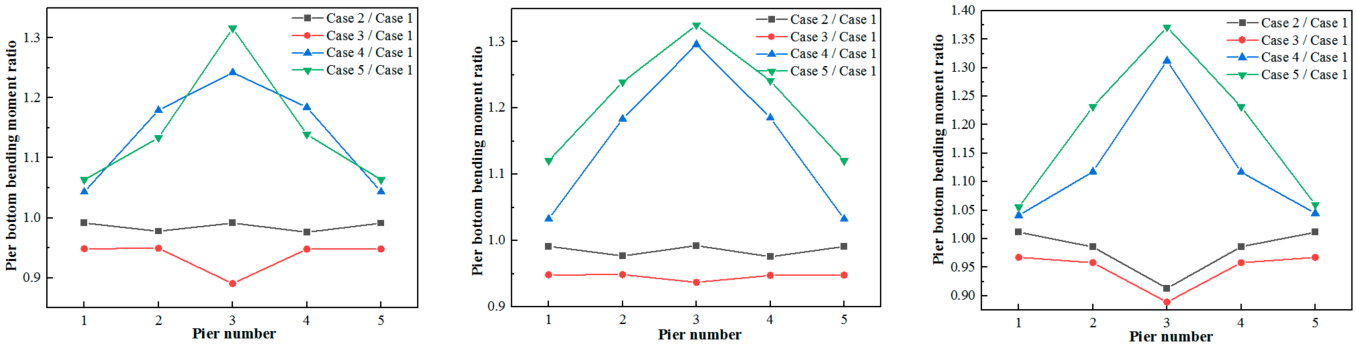

(**a**) 0.1 g (**b**) 0.3 g (**c**) 0.6 g

Figure 7. Bending moment of each case relative to case 1.

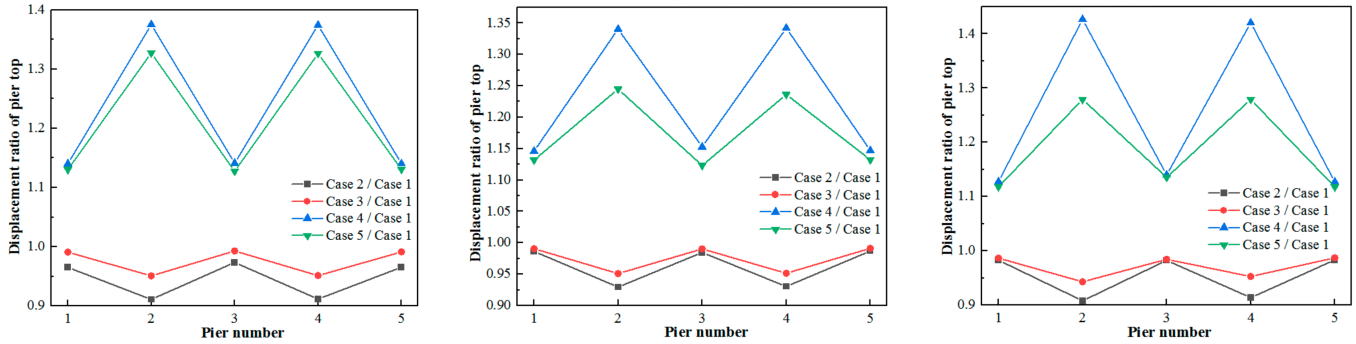

(**a**) 0.1 g (**b**) 0.3 g (**c**) 0.6 g

Figure 8. Displacement ratio of the pier tops of each case to case 1.

(3) Bearing displacement

The deformation law of the bearings is basically the same under the action of the different seismic intensities. Here, only the responses of the 1#, 3#, and 13# bearings when the PGA was 0.6 g are analyzed, as shown in Figure 9a–c. It can be seen that comparing case 1 to case 5, when considering the influence of temperature on the concrete material properties of the bridge pier and the bearing stiffness, the resulting bearing displacement changes significantly compared with the normal temperature, and the bearing displacement of each case was as follows: case 3 > case 2 > case 1 > case 4 > case 5. Under the same seismic excitation, the seismic response law of the 1#, 3#, and 13# bearings was basically the same. When only considering the influence of extreme temperature on the mechanical parameters of the plate rubber bearing, it can be seen from the comparison of the working conditions 1, 2, and 4 that, under the same intensity of seismic excitation, with the decrease in temperature the shear stiffness increased gradually due to the shearing of the rubber bearing, which leads to the gradual weakening of the deformation capacity of the bearing. Compared with the normal temperature condition (condition 1), the peak displacement of the bearing under the extreme high temperature condition (condition 2) increased by 13.20% at most, while at the extreme low temperature the peak displacement of the bearing under the extreme low temperature condition (condition 4) was 11.77% smaller than that under the normal temperature working condition (condition 1). When considering the influence of extreme temperature on the mechanical properties of the piers and bearings at the same time, the peak displacement of the bearings in the extreme high temperature case (case 3) increased by 16.31% compared with the normal temperature case, while the peak displacement of the bearings in the extreme low temperature case (Case 5) decreased by 14.54% compared with the normal temperature case under the same seismic excitation.

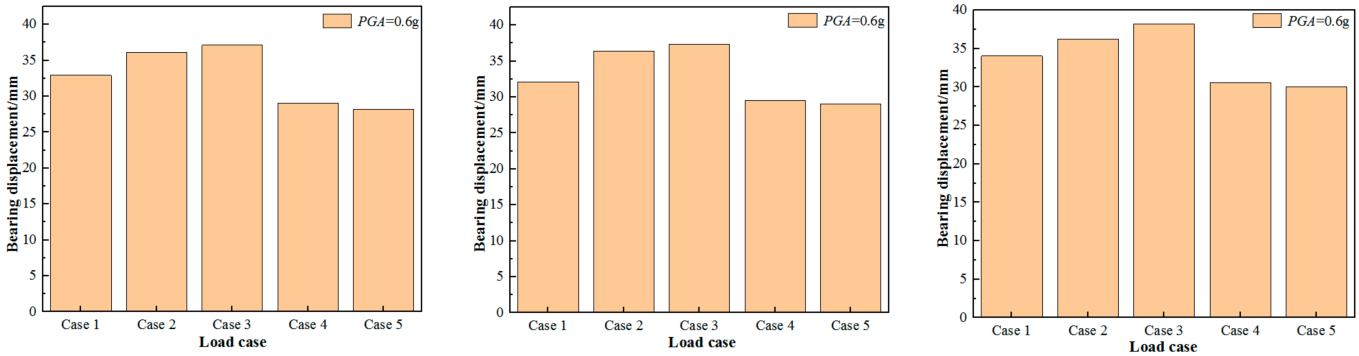

(**a**) 1#Bearing (**b**) 3#Bearing (**c**) 13#Bearing

Figure 9. Bearing displacement.

4.3. Seismic Response Analysis in Cross-Bridge Direction

(1) Pier bottom bending moments

According to the ratio diagram of the pier bottom bending moments under extreme temperature and normal temperature conditions under transverse seismic action of the bridge (Figure 10), the response of the pier bottom moment of each pier is basically the same as the seismic response law under the seismic action in the direction of the bridge, and the overall performance is as follows: extreme low temperature condition (conditions 4, 5) > normal temperature condition (condition 1) > extreme high temperature condition (conditions 2, 3), and the pier bottom moment of the bridge pier shows a negative correlation with temperature. When only considering the influence of the mechanical characteristics of the rubber bearings under extreme temperatures on the seismic performance of the bridge, due to the decrease in temperature the bearing stiffness increased, resulting in the increase in the stiffness of the connection between the pier and the upper part, which increased the maximum bending moment at the bottom of the pier under the extreme low temperature condition (condition 4) by 10.38% compared with that under the normal temperature condition (condition 1). At the PGA of 0.1 g, the change in moment at the bottom of the 3# intersection pier compared with the other piers is relatively obvious, and the maximum change in the moment response under extreme low temperature conditions was 12.59% compared with normal temperature conditions. Meanwhile, on the other piers, the relative difference in moment response under different temperature conditions did not exceed 10% compared with the normal temperature conditions. At the PGA of 0.3 g, the relative difference between pier 2# and pier 4# in the extreme low temperature working condition was 13.28% compared with the normal temperature working condition, while the difference between the other piers was smaller. At the PGA of 0.6 g, the maximum difference in the bending moment response of each pier in the extreme low temperature condition was 8.74% compared to the room temperature condition, and the difference in the extreme high temperature condition was no more than 5%. It can be seen that at the extreme low temperature, the moment response of each pier changes significantly compared with the normal temperature state.

(2) Displacement of pier tops

From the pier top displacement ratio diagram (Figure 11) obtained under the extreme temperature and normal temperature conditions of the bridge under the lateral earthquake action, it can be seen that, comparing case 1 to case 5 and due to the influence of temperature on the concrete material properties of the bridge pier and the mechanical properties of the bearings, the connection stiffness between the bridge pier and the beam was changed, the displacement of each bearing was restrained in the transverse direction, the overall performance was: case 4 > case 5 > case 1 > case 3 > case 2, and the transverse pier top displacement of the bridge pier was negatively correlated with the temperature. When considering the influence of extreme temperature on the mechanical properties of the

piers and bearings, the maximum reduction in pier top displacement under the extreme high temperature condition (case 3) was 12.94% compared with the normal temperature condition (case 1), while the maximum increase in pier top displacement under the extreme low temperature condition (case 5) was 11.40% compared with the normal temperature condition (Case 1) under different seismic excitations. When the ground motion intensity was the same, the high temperature causes the reduction of pier stiffness, which in turn causes the pier top displacement of each pier to increase significantly, while the low temperature results in a decreasing trend. Under the effect of different seismic excitations, the maximum increase in displacement of the pier tops in case 4 compared with case 1 was 11.72%, 13.53%, and 8.34%, respectively, and the maximum decrease in displacement of the pier tops in case 2 compared with case 1 was 6.00%, 11.43% and 8.10%, respectively. In the low temperature environment it can be seen that when the PGA was 0.1 g, the maximum increase in displacement of the pier tops in case 4 compared with case 5 was 6.74%, which is due to the increase in pier stiffness caused by the decrease in temperature.

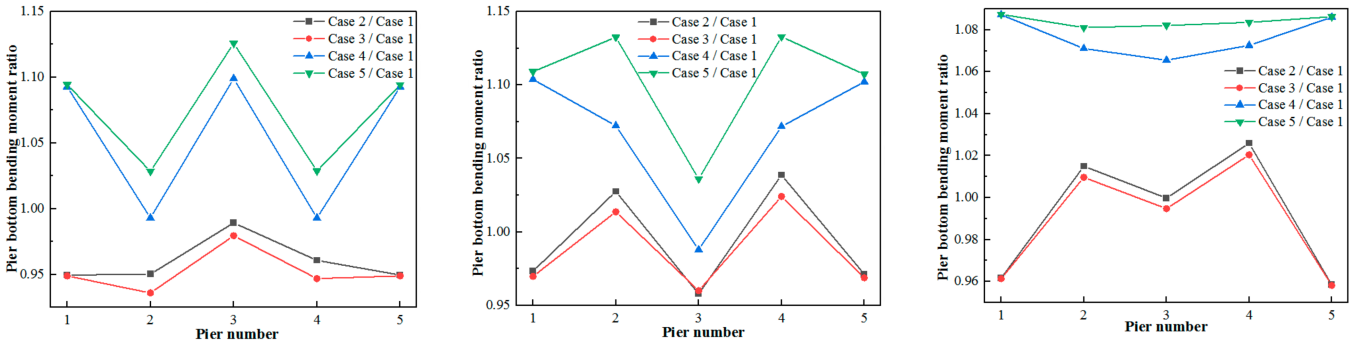

(**a**) 0.10 g (**b**) 0.30 g (**c**) 0.60 g

Figure 10. Bending moment of each case relative to case 1.

(3) Bearing displacement

Under the action of different earthquake intensities, the deformation law of the bearings is basically the same. Here, only the responses of the 1#, 3#, and 13# bearings under the action of a transverse bridge earthquake when the PGA was 0.6 g are analyzed, as shown in Figure 12. Compared with conditions 1~5, the change laws of the cross-bridge bearing displacement and along-bridge bearing displacement are basically the same, showing that case 2 > case 3 > case 1 > case 5 > case 4. When only considering the influence of extreme temperature on the mechanical parameters of the plate rubber bearing, under the same seismic excitation, the peak displacement of the bearing under the extreme high temperature condition was increased by 13.65% compared with the normal temperature condition, while in the extreme low temperature condition the peak displacement of the bearing was reduced by 23.63% compared with the normal temperature condition. Under the same seismic excitation, when considering the influence of extreme temperature on the mechanical properties of the concrete and bearings, the peak displacement of the bearings in the extreme high temperature condition was increased by 12.04% compared with the normal temperature condition, while the peak displacement of the bearings in the extreme low temperature condition was reduced by 22.18% compared with the normal temperature condition.

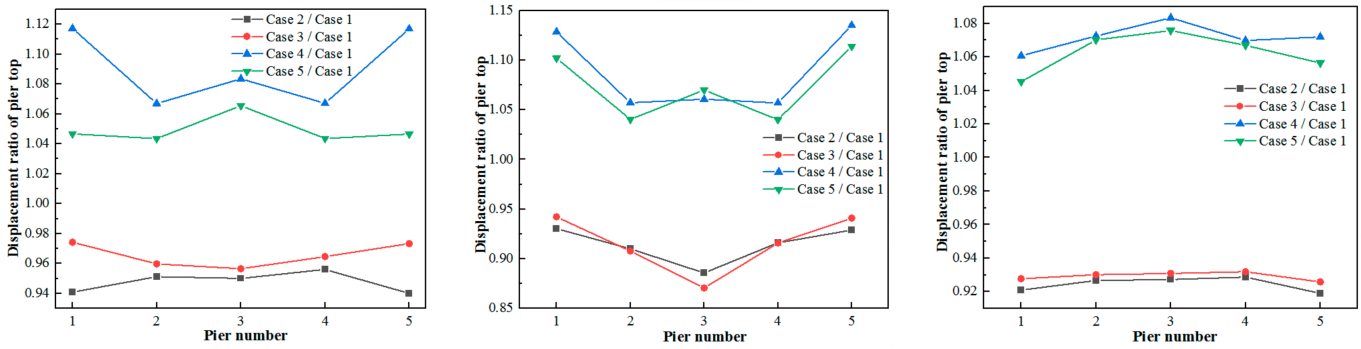

(**a**) 0.10 g (**b**) 0.30 g (**c**) 0.60 g

Figure 11. Displacement ratio of the pier tops of each case relative to case 1.

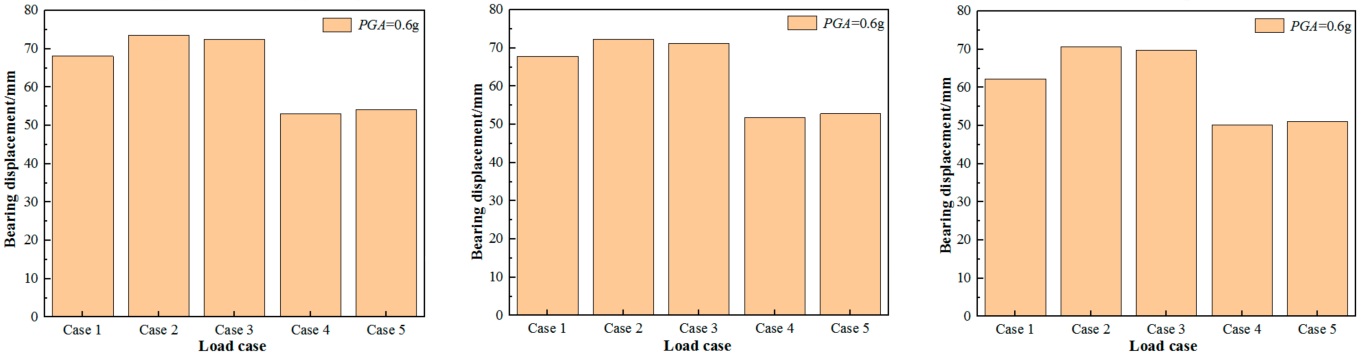

(**a**) 1#Bearing (**b**) 3#Bearing (**c**) 13#Bearing

Figure 12. Bearing displacement.

5. Conclusions

The effect of temperature on the seismic response of continuous girder bridges with LRBs was investigated by considering the effect of extreme temperature on the concrete material properties of the bridge piers and the mechanical properties of the LRBs using a nonlinear time-history analysis. Based on the results of the analysis, the following conclusions are drawn.

The extreme temperatures caused changes in the stiffness of the bearings and material properties of the pier concrete, which increased the internal force and displacement responses of the piers by 37.13% and 32.74%, respectively, in the extreme low temperature conditions compared to normal temperature conditions.

The effect of varying temperature on the mechanical parameters of the LRBs leads to a change in the connection stiffness between the piers and the superstructure. The internal forces and displacements of the bridge piers under seismic action are negatively correlated with temperature, and the bearing displacements are positively correlated with temperature.

The change in the flexural elastic modulus of the bridge piers due to the ambient temperature results in a significant change in the natural frequency of the bridge. The increase in the rigidity of the piers and the stiffness of the bearing connections due to the extreme low temperature is the main reason for the increase in the internal force response of the bridge piers.

The extreme low temperatures increased the stiffness of the piers and bearings, increasing the internal force response of the connecting pier by more than 30% compared to the normal temperature state during the earthquake, and the displacement response of the fixed bearing pier by 42%. Temperature was taken into account in the design.

Author Contributions: Conceptualization, L.W., L.Y., X.D., X.Z. and Z.L.; methodology, L.W., L.Y., X.D., X.Z. and Z.L.; software, L.W., L.Y., X.D. and X.Z.; validation, L.W., L.Y., X.D. and Z.L.; formal analysis, L.W., L.Y., X.D., X.Z. and Z.L.; investigation, L.W., L.Y., X.D. and Z.L.; data curation, L.W., L.Y. and X.Z.; writing—original draft preparation, L.W., L.Y., X.D. and X.Z.; writing—review and editing, L.W., X.D., X.Z. and Z.L.; visualization, L.W., L.Y. and X.D.; supervision, L.Y. and Z.L.; project administration, L.W. and L.Y.; funding acquisition, L.W. All authors have read and agreed to the published version of the manuscript.

Funding: The authors would like to acknowledge the research grant 52068045 received from the National Natural Science Foundation of China, the young doctor support project in Colleges and universities of Gansu Province (grant NO. 2023QB-045) and the Project Supported by the Young Scholars Science Foundation of Lanzhou Jiaotong University (grant NO. 2022055) for the works reported herein. The authors gratefully express their gratitude for the financial support.

Data Availability Statement: Data related to this research are not available for public access.

Conflicts of Interest: The authors declare no conflict of interest.

References

1. Wang, Q.; Zheng, Z.; Qiao, H.; De Domenico, D. Seismic protection of reinforced concrete continuous girder bridges with inerter-based vibration absorbers. *Soil Dyn. Earthq. Eng.* **2023**, *164*, 107526. [CrossRef]
2. Eslamnia, H.; Malekzadeh, H.; Jalali, S.A.; Moghadam, A.S. Seismic energy demands and optimal intensity measures for continuous concrete box-girder bridges. *Soil Dyn. Earthq. Eng.* **2023**, *165*, 107657. [CrossRef]
3. Data-driven rapid damage evaluation for life-cycle seismic assessment of regional reinforced concrete bridges. *Earthq. Eng. Struct. Dyn.* **2022**, *51*, 2730–2751. [CrossRef]
4. Wu, H.J.; Zhang, H.; Lu, P. Brief analysis of temperature effect on the low pier continuous rigid-frame bridge. *Adv. Mater. Res.* **2011**, *255–260*, 911–915. [CrossRef]
5. Hossain, T.; Segura, S.; Okeil, A.M. Structural effects of temperature gradient on a continuous prestressed concrete girder bridge: Analysis and field measurements. *Struct. Infrastruct. Eng.* **2020**, *16*, 1539–1550. [CrossRef]
6. Liu, C.; DeWolf, J.T. Effect of temperature on modal variability for a curved concrete bridge//Smart Structures and Materials 2006: Sensors and Smart Structures Technologies for Civil, Mechanical, and Aerospace Systems. *SPIE* **2006**, *6174*, 1050–1060.
7. Liu, C.; DeWolf, J.T. Effect of temperature on modal variability of a curved concrete bridge under ambient loads. *J. Struct. Eng.* **2007**, *133*, 1742–1751. [CrossRef]
8. Ministry of Transport of the People's Republic of China. *JTG/T 2231-01—2020 Specifications for Seismic Design of Highway Bridges*; China Communications Press: Beijing, China, 2020.
9. Zhang, R.-J.; Li, A.-Q. Experimental study on temperature dependence of mechanical properties of scaled high-performance rubber bearings. *Compos. Part B Eng.* **2020**, *190*, 107932. [CrossRef]
10. Safina, L.; Shuvalov, A.; Kovalev, M. Study of reinforced elastomeric bearings for structures in seismic areas. *MATEC Web Conf.* **2018**, *193*, 03009. [CrossRef]
11. Shuvalov, A.; Safina, L.; Kovalev, M. Experimental research of service actions influence on elastomeric bearings elastic properties. *IOP Conf. Ser. Mater. Sci. Eng.* **2020**, *869*, 052018. [CrossRef]
12. Lev, Y.; Faye, A.; Volokh, K.Y. Experimental study of the effect of temperature on strength and extensibility of rubberlike materials. *Exp. Mech.* **2018**, *58*, 847–858. [CrossRef]
13. Shen, C.-Y.; Huang, X.-Y.; Chen, Y.-Y.; Ma, Y.-H. Factors Affecting the Dependency of Shear Strain of LRB and SHDR: Experimental Study. *Actuators* **2021**, *10*, 98. [CrossRef]
14. Karuk, V.; Çavdar, E.; Özdemir, G. DIŞ ORTAM SICAKLIĞININ ÇİFT ÇEKİRDEKLİ KAUÇUK BİR İZOLATÖR ÖZELLİKLERİ ÜZERİNDEKİ ETKİSİ. In Proceedings of the International Conference on Earthquake Engineering and Seismology (5ICEES), Ankara, Turkey, 8–11 October 2019; Volume 8, p. 11.
15. Amin, N.M.; Alisibramulisi, A.; Kadir, N. Compressive Strength of Laminated Rubber Bearing Due to Different Tem-perature Exposure. In Proceedings of the International Civil and Infrastructure Engineering Conference 2013, Kuching, Malaysia, 22–25 September 2013; Springer: Singapore, 2014; pp. 701–711.
16. Yakut, A.; Yura, J.A. Evaluation of Low-Temperature Test Methods for Elastomeric Bridge Bearings. *J. Bridg. Eng.* **2002**, *7*, 50–56. [CrossRef]
17. Steelman, J.S.; Fahnestock, L.A.; Filipov, E.T.; LaFave, J.M.; Hajjar, J.F.; Foutch, D.A. Shear and Friction Response of Nonseismic Laminated Elastomeric Bridge Bearings Subject to Seismic Demands. *J. Bridg. Eng.* **2013**, *18*, 612–623. [CrossRef]
18. Yakut, A.; Yura, J.A. Parameters Influencing Performance of Elastomeric Bearings at Low Temperatures. *J. Struct. Eng.* **2002**, *128*, 986–994. [CrossRef]
19. Strauss, A.; Apostolidi, E.; Zimmermann, T.; Gerhaher, U.; Dritsos, S. Experimental investigations of fiber and steel reinforced elastomeric bearings: Shear modulus and damping coefficient. *Eng. Struct.* **2014**, *75*, 402–413. [CrossRef]

20. Du, Y.; Li, H.; Ma, Y.; Jin, J. Behaviour of laminated rubber bearing under low and its effect on the dynamic reliability of isolated structure. In Proceedings of the International Conference on Earthquake Engineering, Taipei, Taiwan, 12–13 October 2006.
21. Billah, A.M.; Todorov, B. Effects of subfreezing temperature on the seismic response of lead rubber bearing isolated bridge. *Soil Dyn. Earthq. Eng.* **2019**, *126*, 105814. [CrossRef]
22. Xu, G.; Guo, T.; Li, A.; Zhang, R.; Zhu, R.; Liu, F. Influence of ambient temperature on seismic performance of elastomeric isolation structural system. *Structures* **2023**, *55*, 1763–1773. [CrossRef]
23. Wang, S.; Tan, P.; Yuan, Y.; Zheng, W.; Jin, S.; Xu, X. Efficacy of 3M-PTGL on low-temperature seismic performance of polyurethane elastomeric bearings for bridges. *Eng. Struct.* **2023**, *294*, 116703. [CrossRef]
24. Li, Y.; Zhai, Y.; Liang, W.; Li, Y.; Dong, Q.; Meng, F. Dynamic mechanical properties and visco-elastic damage constitutive model of freeze-thawed concrete. *Materials* **2020**, *13*, 4056. [CrossRef]
25. Krishna, D.A.; Priyadarsini, R.S.; Narayanan, S. Effect of elevated temperatures on the mechanical properties of concrete. *Procedia Struct. Integr.* **2019**, *14*, 384–394. [CrossRef]
26. Xie, J.; Li, X.; Wu, H. Experimental study on the axial-compression performance of concrete at cryogenic temperatures. *Constr. Build. Mater.* **2014**, *72*, 380–388. [CrossRef]
27. Xie, J.; Yan, J.-B. Experimental studies and analysis on compressive strength of normal-weight concrete at low temperatures. *Struct. Concr.* **2017**, *19*, 1235–1244. [CrossRef]
28. Li, X.; Xie, J.; Wu, H.H. Experimental research on the constitutive relationship of concrete in a cryogenic environment. *Eng. Mech.* **2014**, *31*, 195–200. [CrossRef]
29. Yan, J.-B.; Cao, J.; Xie, P.; Xie, J. Concrete-filled circular stainless-steel tubular columns subjected to low-temperature axial compression. *Structures* **2023**, *55*, 916–932. [CrossRef]
30. Ministry of Housing and Urban Rural Development of the People's Republic of China. *GB 51081-2015 Technical Code for Application of Concrete under Cryogenic Circumstance*; China Planning Press: Beijing, China, 2015.
31. Xie, J.; Lei, G.-C.; Wei, Q.; Han, X.-D. Experimental research on flexural properties of reinforced concrete beams at cryogenic temperatures. *J. Build. Struct.* **2014**, *35*, 65–71. [CrossRef]
32. Rostásy, F.; Wiedemann, G. Stress-strain-behaviour of concrete at extremely low temperature. *Cem. Concr. Res.* **1980**, *10*, 565–572. [CrossRef]
33. Guo, Z. The Strength and Deformation Test of Concrete—Experimental Basis and the Constitutive Relation. Ph.D. Thesis, Tsinghua University Press, Beijing, China, 1997; pp. 31–35.
34. Yan, J.-B.; Xie, J. Experimental studies on mechanical properties of steel reinforcements under cryogenic temperatures. *Constr. Build. Mater.* **2017**, *151*, 661–672. [CrossRef]
35. Xie, J.; Han, X.D.; Pei, J.M.; Lei, G.D. Experimental study of mechanical properties of reinforcing steels at cryogenic temper-atures. *Ind. Constr.* **2015**, *45*, 126–129+172. [CrossRef]
36. Zhuang, J. *Qiao Liang Zhi Zuo*; China Railway Publishing House: Beijing, China, 2015.
37. Park, J.Y.; Jang, K.-S.; Lee, H.-P.; Lee, Y.H.; Kim, H. Experimental Study on the Temperature Dependency of Full Scale Low Hardness Lead Rubber Bearing. *J. Comput. Struct. Eng. Inst. Korea* **2012**, *25*, 533–540. [CrossRef]
38. Ministry of Communications of the People's Republic of China. *JT/T 4—2019 Laminated Bearing for Highway Bridge*; China Communications Press: Beijing, China, 2019.
39. State Seismological Bureau/Ministry of construction. *GB 18306-2015 Seismic Ground Motion Parameter Zoning Map of China*; China Standards Press: Beijing, China, 2015.